



## A molecular “screw-clamp”: accelerating click reactions in miniemulsions†

Evandro M. Alexandrino,<sup>a</sup> Philipp Buchold,<sup>a</sup> Manfred Wagner,<sup>a</sup> Adrian Fuchs,<sup>a</sup> Andreas Kreyes,<sup>a</sup> Clemens K. Weiss,<sup>ab</sup> Katharina Landfester<sup>a</sup> and Frederik R. Wurm<sup>\*a</sup>

Cite this: *Chem. Commun.*, 2014, 50, 10495

Received 29th May 2014,  
Accepted 17th July 2014

DOI: 10.1039/c4cc04119d

www.rsc.org/chemcomm

**The interface as a “screw clamp”: the copper-free 1,3-dipolar azide–alkyne cycloaddition at the interface of nanodroplets in miniemulsions was studied in detail by NMR spectroscopic methods. The reaction at the oil–water interface proved to exhibit higher rate constants, increased molecular weights and high regioregularity compared to the reaction in solution.**

The 1,3-dipolar Huisgen cycloaddition between alkynes and azides (AAC) is certainly the most successful and widespread type of ‘click’ reaction resulting in the formation of 1,2,3-triazoles.<sup>1</sup> The reaction developed by Huisgen was originally a thermally activated relatively slow reaction, which generated a mixture of two regioisomers: 1,4- and 1,5-disubstituted 1,2,3-triazoles.<sup>2</sup> Later, Sharpless and coworkers<sup>3</sup> and Medal and coworkers<sup>4</sup> obtained regioselective products (1,4-disubstituted 1,2,3-triazoles) with high yields by the use of copper catalysts under mild conditions. Ruthenium catalysts have also been used for the preparation of 1,5-disubstituted 1,2,3 triazoles<sup>5</sup> and recently iridium for the preparation of regioselective products from electron rich internal alkynes.<sup>1</sup> The removal of these metal catalysts however can be challenging especially for biological applications.<sup>6,7</sup> Some approaches to metal-free AAC have been successfully developed including strained cyclooctynes,<sup>7,8</sup> activated alkynes<sup>7,9</sup> and electron deficient alkynes.<sup>7,10,11</sup> Concerning the various alkyne derivatives, the electron deficient propiolates are of special interest due to the straightforward esterification of the alcohol of choice with propiolic acid.<sup>10</sup>

The absence of a catalyst and the bioorthogonal functional groups makes this reaction highly suitable for the preparation of materials for biomedical applications, *e.g.* the formation of bioconjugates, nanocarriers, or biodegradable surfactants. To obtain reasonable reaction rates however, elevated temperatures are still necessary, which may for example denature biomolecules.

Another interesting aspect of this reaction is the feasible combination of two immiscible reactants *via* an interfacial click reaction to either generate a polymeric shell or an amphiphilic material like a surfactant, *via* orthogonal chemistry.

This work explores the possibilities of the copper-free click reaction between azides and electron deficient propiolates at the droplet interface of a stable miniemulsion. First, we investigate the effect on reaction kinetics of an A<sub>2</sub> + B<sub>2</sub> polyaddition with respect to conversion and molecular weights. The resulting polyesters are also compared to solution protocols at different temperatures. Further, the droplet interface is used to generate a surfactant *via* an *in situ* click reaction. The resulting stabilized miniemulsion could be further employed in the radical polymerization of styrene. In the miniemulsion, droplets with a very high total surface area in comparison to conventional emulsions or a homogeneous reaction system are generated.<sup>12</sup> These monodisperse droplets can be used as nanocontainers for reactions inside or at the interface of the droplets.<sup>12</sup>

The kinetics of the reaction and the structural features of both systems were characterized in detail by various NMR spectroscopic techniques and gel permeation chromatography (GPC). Previously, our group has successfully developed a facile method to produce nanocapsules by copper-free click polymerization for encapsulation of functional molecules using a water soluble azide (2,2-bis-(azidomethyl)propan-1,3-diol, BAP) and an organic soluble alkyne (hexane-1,6-diyl dipropiolate, HDDP).<sup>13</sup> Following these results, the detailed kinetic investigation of the copper-free click reaction at the interface of a miniemulsion was studied. Further, the polymerization of HDDP and BAP at the interface and the use of this methodology to synthesize amphiphilic molecules, like surfactants, were also achieved (Scheme 1).

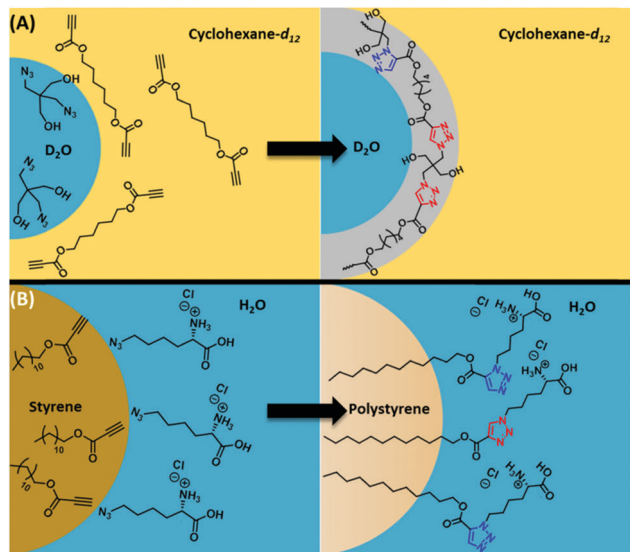
<sup>1</sup>H NMR spectroscopy was used for the *in situ* measurement of the polymerization kinetics<sup>14</sup> over a period of 800 min for the various reactions. Both solution and inverse miniemulsion polymerizations were carried out in either DMSO-*d*<sub>6</sub> or cyclohexane-*d*<sub>12</sub> as a continuous phase and D<sub>2</sub>O as a dispersed phase respectively. Temperatures of 298 K and 323 K with a delay time of approximately 8 min between each spectral acquisition were used (see Fig. S3–S6, ESI† for an overlay of different <sup>1</sup>H NMR

<sup>a</sup> Max Planck Institute for Polymer Research, Ackermannweg 10, 55128, Mainz, Germany. E-mail: wurm@mpip-mainz.mpg.de

<sup>b</sup> University of Applied Sciences Bingen, Berlinstrasse 109, 55411 Bingen, Germany

† Electronic supplementary information (ESI) available. See DOI: 10.1039/c4cc04119d





**Scheme 1** Polyadditions performed at the interface: (A) the system used for evaluating the kinetics of polymerization between HDDP and BAP in an inverse miniemulsion (cyclohexane-*d*<sub>12</sub>/D<sub>2</sub>O); (B) *in situ* surfactant formation using the click reaction to stabilize a direct miniemulsion (water–styrene) during radical polymerization of polystyrene nanoparticles. The different possible regioisomers 1,4- and 1,5-disubstituted 1,2,3-triazoles are highlighted here in red and blue, respectively.

spectra of the polymerizations). The evolution of the integral of the alkyne proton was followed over time in comparison to an internal standard (0.07 ppm from decamethylcyclotriasiloxane). The results of the consumption of HDDP over time are plotted in Fig. 1.

As can be seen from Fig. 1, the miniemulsion system resulted in a faster consumption of the HDDP monomer in comparison to solution polymerization. Considering the system as a second order reaction, the following method can be applied to obtain the values of  $k_2$ :<sup>15</sup>

$$\frac{1}{1-x} = k_2 t, \text{ with } x = 1 - \frac{[\text{HDDP}]}{[\text{HDDP}]_0} \quad (1)$$

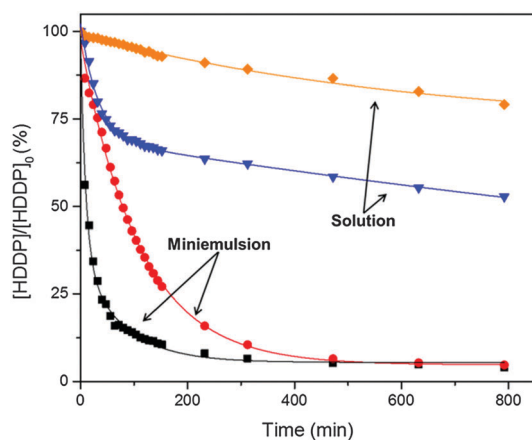


**Fig. 1** Conversion of HDDP for the polyaddition with BAP in miniemulsion (water–cyclohexane  $c = 1.94 \times 10^{-2} \text{ mol L}^{-1}$ ) at 323 K (■) and 298 K (●) and in solution (DMSO-*d*<sub>6</sub>,  $c = 2.76 \times 10^{-2} \text{ mol L}^{-1}$ ) at 323 K (▼) and 298 K (◆), as determined by <sup>1</sup>H NMR.

Applying this equation across the different reaction conditions for the first hour (Fig. S7, ESI<sup>†</sup>), at 298 K, the miniemulsion polymerization system showed a 25-fold increase in the value of  $k_2$  compared to solution polymerization. At 323 K a 12-fold increase was measured. The increase in the rate of the reaction can be explained in terms of the so-called “pseudo-phase model”, which relates the partitioning of monomers at the interface to the characteristics of the reagents with both solvents.<sup>16,17</sup> Bravo-Díaz and Romsted have modelled the reactivity of “macro”emulsions and “micro”emulsions in terms of the pseudo-phase model.<sup>17</sup> Miniemulsions are kinetically stable systems, similar to macroemulsions, however with the additional kinetic stabilization against diffusion and collisions. The system studied herein uses a non-ionic surfactant, which avoids the interference of charges in the kinetics of the reaction, as observed by Engberts and coworkers for the kinetics of cycloadditions in microemulsions.<sup>18</sup> Thus, this system is a better comparison to solution polymerization. Two assumptions have been made for the application of the pseudo-phase model:

(a) the distribution of the components is a thermodynamic equilibrium, which can be represented by the partition coefficient;

(b) the interfacial region is in a dynamic equilibrium state.<sup>17</sup>

The partition coefficient depends on the solubility of the components in each of the solvents; therefore the level of acceleration observed will be directly linked to the chemical properties of the components of the system.

As an additional factor, two reaction temperatures were examined: for miniemulsion polymerization, an increase in the  $k_2$ -value from 298 K to 323 K of approximately 7-fold and for solution polymerization an increase of approximately 15-fold were observed. This difference can be rationalized in terms of mobility. The increase of the temperature directly affects the Brownian mobility of the molecules in the system. In a miniemulsion system one monomer is confined inside the droplet and has limited space and therefore limited mobility at the interface, while in the homogeneous reaction both monomers have a similar mobility and are thus significantly more influenced by temperature variations.

The evolution of the molecular weight for both polymerization methods was followed by GPC (see Table S2 and Fig. S12, ESI<sup>†</sup>). The data highlight that higher molecular weights are achieved in the miniemulsion systems at both temperatures compared to solution polymerizations. This may be explained by considering two factors: (1) in solution the overall concentration is lower than at the interface of nanodroplets resulting in a decreased molecular weight of the polymer (up to  $M_w = 4500 \text{ g mol}^{-1}$  (vs. PS)); and (2) in the heterophase system, the polymer precipitates, and is confined to the interface resulting in higher conversions and molecular weights (up to  $M_w = 10\,000 \text{ g mol}^{-1}$  in miniemulsion at 323 K). The final morphology obtained from the miniemulsion systems is, as expected, the formation of nanocapsules with a mean diameter of  $190 \pm 60 \text{ nm}$ . This could be confirmed by SEM, TEM and light scattering measurements (see Fig. S13 and S14, ESI<sup>†</sup>) and agrees well with what has been previously reported by our group.<sup>13</sup>

An interesting aspect of the interfacial reaction is whether there is an influence on the microstructure of the polymer. Tang and coworkers<sup>10</sup> have used metal-free alkyne-azide polymerization



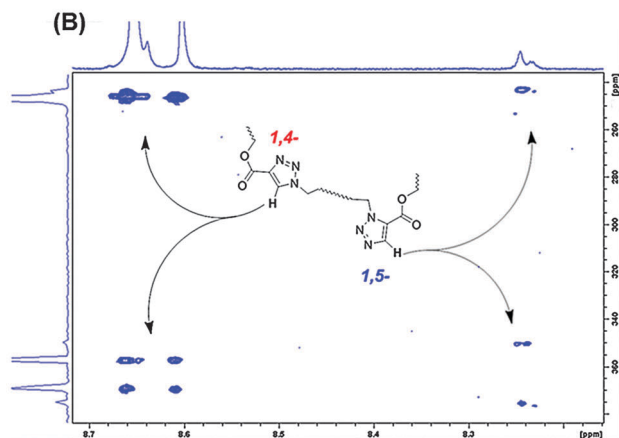
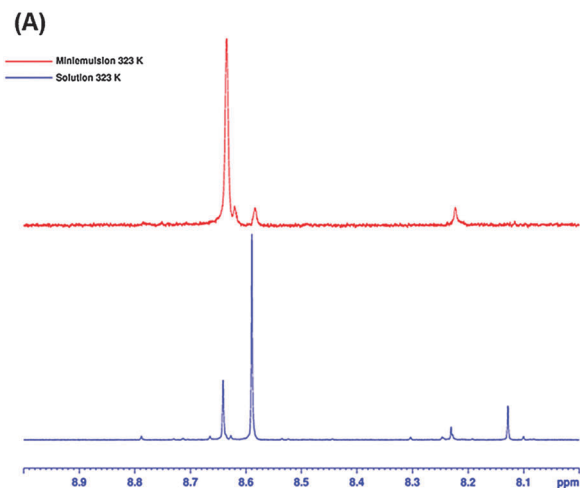


Fig. 2 (A)  $^1\text{H}$  NMR spectra in  $\text{DMSO-}d_6$  (700 MHz, Avance III) from the triazole proton region for the product of polymerization in miniemulsion (red) and in solution (blue) at 323 K; (B) 2D  $^1\text{H-}^{15}\text{N}$  HMBC (850 MHz, Avance III) analysis of the polymer obtained by miniemulsion polymerization at 323 K in  $\text{DMSO-}d_6$ . The upper spectrum corresponds to the  $^1\text{H}$  spectrum, the spectrum on the left is the internal calculation of the cross peaks in the  $^{15}\text{N}$ -frequency range.

to produce a series of polymers with diazides and dipropiolates in solution and found a high tendency for the formation of 1,4-triazoles (over 90%). Both possible regioisomers (1,4- and 1,5-triazole) can be differentiated by two distinct singlets between 7 and 10 ppm in the  $^1\text{H}$  NMR spectrum.<sup>19</sup> Both products of polymerization in solution and in miniemulsion were analysed *via*  $^1\text{H}$  NMR spectroscopy ( $\text{DMSO-}d_6$ ) and several signals can be detected in the triazole region (Fig. 2(A)). Interestingly, an inversion in the relative intensities of these peaks is observed depending on the polymerization methodology. Previously,  $^1\text{H-}^{15}\text{N}$  HMBC (heteronuclear multiple bond correlation) NMR spectroscopy was used as a powerful tool to distinguish different triazole isomers.<sup>19</sup> The  $^1\text{H-}^{15}\text{N}$  HMBC analysis of the polymer obtained by miniemulsion polymerization is shown in Fig. 2(B). As can be clearly seen from the H–N correlation, the signals between 8.6 and 8.7 ppm (in the H NMR) are related to the same regioisomer, while the two signals around 8.24 ppm correlate with each other. The values are in agreement with the values observed by Alfonso and coworkers<sup>19</sup> and indicated that the three signals at lower field of

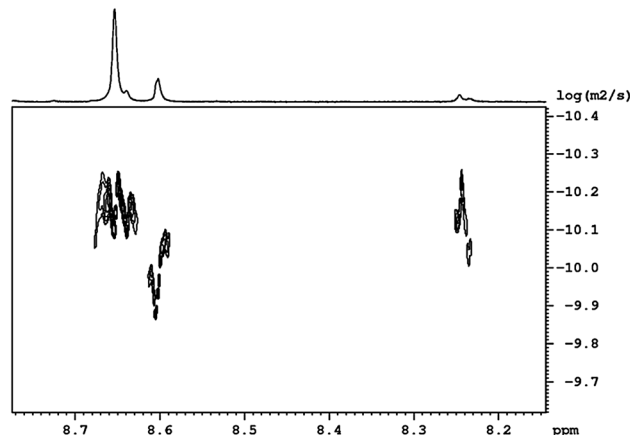


Fig. 3 DOSY  $^1\text{H}$ -NMR (850 MHz, Avance III) measurement for the product of miniemulsion polymerization at 323 K in  $\text{DMSO-}d_6$ .

the spectrum stem from the 1,4-disubstituted 1,2,3-triazoles, while the two signal at higher field correspond to the 1,5-disubstituted 1,2,3-triazole derivatives. Miniemulsion thus preferentially produces the 1,4-triazole regioselective polymer (approximately 91%). Solution polymerization also predominates with the 1,4-isomer, however it appears to be of a different 1,4-species.

To elucidate the nature of this second 1,4-derivative (8.65 ppm and 8.61 ppm), diffusion-ordered NMR spectroscopy (DOSY)  $^1\text{H}$ -NMR analysis was performed. Fig. 3 shows the spectrum of the product of miniemulsion polymerization at 323 K. The diffusion coefficient for the signal at *ca.* 8.61 ppm is higher (approximately  $9.0 \times 10^{-11} \text{ m}^2 \text{ s}^{-1}$ ) than the one observed for the other peaks (approximately  $5.5 \times 10^{-11} \text{ m}^2 \text{ s}^{-1}$ ). The fact that the peaks have a well-defined shape suggests that it originates from a smaller, faster diffusing species of defined architecture and one that is not related to the molecular weight distribution of the polymer. A plausible explanation is the formation of cyclic oligomers. Considering the surface curvature of the droplet and the lower mobility of the reactants after precipitation at the interface, a lower probability for the formation of cyclic structures for miniemulsion polymerization in comparison to solution polymerization is expected. This assumption is in agreement with the change in the intensity between both methods observed in the 1D- $^1\text{H}$  NMR (Fig. 2(A)).

The miniemulsion polyaddition is a clear example of the interfacial “screw clamp” and has the potential to accelerate certain reactions under mild conditions to give an easy pathway for the formation of amphiphilic molecules as protein conjugates or surfactants. To further exemplify this effect and the use of this approach in the preparation of amphiphilic molecules, a monofunctional system was used to generate a surfactant *in situ*, under mild conditions with the capability to stabilize a direct miniemulsion polymerization system. This is the first example of a chemical reaction that can be applied *in situ* to generate a surfactant that stabilizes a miniemulsion of monomer droplets for instantaneous polymerization. Previously, aliphatic carboxylic acids were deprotonated in the heterophase to generate ionic surfactants<sup>20,21</sup> while metallosurfactants and transition metal acetyl acetonates have also been produced *in situ*.<sup>22,23</sup> The generation of a surfactant



*in situ* can have advantages such as faster stabilization of the (mini)emulsion and less secondary nucleation processes.<sup>24</sup> Here, we used the interfacial “screw clamp” for mediating a click reaction in a direct miniemulsion between dodecyl propiolate dispersed in styrene as the organic phase and *N*-ε-azido-L-lysine hydrochloride dissolved in the aqueous phase. The emulsion was produced by stirring and the subsequent application of ultrasound. The nanodroplets were formed with a high surface area and stabilized at the same time by the *in situ* generated, *i.e.* “clicked”, surfactant (compare Scheme 1(B)). After the addition of a radical initiator (VA044) to the aqueous phase, a stable polystyrene nanoparticle dispersion with a mean diameter of *ca.* 300 nm was obtained (Fig. S15, ESI†).

Aqueous miniemulsion was used as a synthetic tool to mediate the metal-free 1,3-dipolar cycloaddition between propiolates and azides. A detailed kinetic investigation *via* NMR spectroscopy was conducted for the copper-free click polyaddition between HDDP and BAP. This A<sub>2</sub> + B<sub>2</sub> polyaddition was studied both in solution and in a biphasic system, *i.e.* miniemulsion, with one monomer being confined in the dispersed phase (water) and the second being dissolved in the continuous phase. Conducting the reaction in miniemulsion leads to a significant acceleration of the reaction leading to higher molecular weights at lower temperatures compared to the reaction in solution. Detailed NMR analyses of the microstructure of the final materials indicated that the polyaddition at the interface of miniemulsion droplets leads to the probable formation of less cyclic oligomers and a high regioselectivity towards the 1,4-triazole isomers.

The catalyst-free 1,3-dipolar cycloaddition in the heterophase can be a powerful tool for bioapplications, *e.g.* the encapsulation or bioconjugation of temperature sensitive biomolecules, such as proteins, that can be mediated at the water interface. Herein, we also used the interfacial “screw clamp” to generate a surfactant *in situ* as an example capable of stabilizing styrene nanodroplets, which could subsequently undergo radical polymerization.

We believe that this approach is especially useful for biological materials due to bioorthogonality, mild conditions (low temperature and no catalyst) and the tolerance to water.

## Notes and references

- 1 S. Ding, G. Jia and J. Sun, *Angew. Chem., Int. Ed.*, 2014, **53**, 1877–1880.
- 2 R. Huisgen, *Angew. Chem., Int. Ed.*, 1963, **2**, 633–645.
- 3 V. V. Rostovtsev, L. G. Green, V. V. Fokin and K. B. Sharpless, *Angew. Chem., Int. Ed.*, 2002, **41**, 2596–2599.
- 4 C. W. Tornøe, C. Christensen and M. Meldal, *J. Org. Chem.*, 2002, **67**, 3057–3064.
- 5 L. Zhang, X. Chen, P. Xue, H. H. Y. Sun, I. D. Williams, K. B. Sharpless, V. V. Fokin and G. Jia, *J. Am. Chem. Soc.*, 2005, **127**, 15998–15999.
- 6 J. F. Lutz, *Angew. Chem., Int. Ed.*, 2008, **47**, 2182–2184.
- 7 C. R. Becer, R. Hoogenboom and U. S. Schubert, *Angew. Chem., Int. Ed.*, 2009, **48**, 4900–4908.
- 8 N. J. Agard, J. A. Prescher and C. R. Bertozzi, *J. Am. Chem. Soc.*, 2004, **126**, 15046–15047.
- 9 S. Sawoo, P. Dutta, A. Chakraborty, R. Mukhopadhyay, O. Bouloussa and A. Sarkar, *Chem. Commun.*, 2008, 5957–5959.
- 10 H. Li, J. Wang, J. Z. Sun, R. Hu, A. Qin and B. Z. Tang, *Polym. Chem.*, 2012, **3**, 1075–1083.
- 11 S. S. van Berkel, A. J. Dirks, S. A. Meeuwissen, D. L. L. Pingen, O. C. Boerman, P. Laverman, F. L. van Delft, J. J. L. M. Cornelissen and F. P. J. T. Rutjes, *ChemBioChem*, 2008, **9**, 1805–1815.
- 12 K. Landfester, *Angew. Chem., Int. Ed.*, 2009, **48**, 4488–4507.
- 13 J. M. Siebert, G. Baier, A. Musyanovych and K. Landfester, *Chem. Commun.*, 2012, **48**, 5470–5472.
- 14 C. Tonhauser, A. Alkan, M. Schömer, C. Dingels, S. Ritz, V. Mailänder, H. Frey and F. R. Wurm, *Macromolecules*, 2013, **46**, 647–655.
- 15 X. Liu, P. Du, L. Liu, Z. Zheng, X. Wang, T. Joncheray and Y. Zhang, *Polym. Bull.*, 2013, **70**, 2319–2335.
- 16 Q. Gu, C. Bravo-Díaz and L. S. Romsted, *J. Colloid Interface Sci.*, 2013, **400**, 41–48.
- 17 L. S. Romsted and C. Bravo-Díaz, *Curr. Opin. Colloid Interface Sci.*, 2013, **18**, 3–14.
- 18 J. B. F. N. Engberts, E. Fernández, L. García-Río and J. R. Leis, *J. Org. Chem.*, 2006, **71**, 6118–6123.
- 19 M. Corredor, J. Bujons, A. Messegueur and I. Alfonso, *Org. Biomol. Chem.*, 2013, **11**, 7318–7325.
- 20 U. El-Jaby, M. Cunningham and T. F. L. McKenna, *Macromol. Chem. Phys.*, 2010, **211**, 1377–1386.
- 21 G. Yi, L. T. Victoria, S. R. S. Ting and B. Z. Per, *Polym. J.*, 2012, **44**, 375–381.
- 22 C. R. van den Brom, M. Wagner, V. Enkelmann, K. Landfester and C. K. Weiss, *Langmuir*, 2010, **26**, 15794–15801.
- 23 C. R. van den Brom, N. Vogel, C. P. Hauser, S. Goerres, M. Wagner, K. Landfester and C. K. Weiss, *Langmuir*, 2011, **27**, 8044–8053.
- 24 U. El-Jaby, M. Cunningham and T. F. L. McKenna, *Macromol. Rapid Commun.*, 2010, **31**, 558–562.

